



# Cool stellar atmospheres with PHOENIX

P. Hauschildt<sup>1</sup> and E. Baron<sup>2</sup>

<sup>1</sup> Hamburger Sternwarte, Gojenbergsweg 112, 21029 Hamburg, Germany; yeti@hs.uni-hamburg.de

<sup>2</sup> Dept. of Physics and Astronomy, University of Oklahoma, 440 W. Brooks, Rm 131, Norman, OK 73019 USA e-mail: baron@nhn.ou.edu

**Abstract.** We give an overview about the state-of-the-art in cool stellar (and sub-stellar) atmosphere simulations. Recent developments in numerical methods and parallel supercomputers, as well as in the quality of input data such as atomic and molecular line lists have led to substantial improvements in the quality of synthetic spectra when compared to multi-wavelength observations. A wide range of objects from M dwarfs and giants down to substellar objects is considered. We discuss effects such as atomic and molecular NLTE (and) line blanketing, external irradiation, and formation and opacities of dust particles and clouds; each of which affects the structure of the atmospheres and their spectra. Current models can simultaneously fit many of the observed features of a given star with a single model atmosphere, however, a number of problems remain unsolved and will have to be addressed in the future, in particular for very low mass stars and substellar objects.

**Key words.** Stellar Atmospheres, Giants, numerical algorithms

## 1. Introduction

Stellar atmosphere modeling has experienced a renaissance in the past decade with the advent of better algorithms and faster computers. This has allowed research groups to remove or relax many of the “standard” assumptions that were made in the 70s and 80s and that had become accepted wisdom over the years. Surprisingly (or not) the new calculations show that many of these assumptions are actually quite bad and can lead to spurious results or incorrect interpretations of observed spectra. The intricate connection between geometry (plane parallel or spherical), line blanketing (atomic and/or molecular) and non-LTE effects (using small to extremely large model atoms and molecules) began to emerge slowly as crucial ingredients for physically correct and meaningful in-

terpretations and analyses of stellar spectra. Unfortunately, easy and simple solutions do not really work for stellar atmospheres (although everybody likes the easy way out and some of them are useful for teaching purposes) and have actually hindered progress and reduced the reliability of results.

New observational techniques opened and continue to open up new areas of stellar atmosphere research. The most important advance has been detailed observations of very low mass stars and after decades of searching, brown dwarfs and extrasolar giant planets. Modeling these objects requires sophisticated stellar atmosphere type modeling with complex equations of state and 100’s of millions of molecular spectral lines in order to even approximately reproduce the observed spectra.

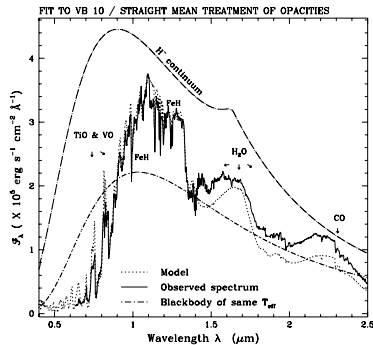


**Fig. 1.** Best fit of Allard & Hauschildt (1995b) to the spectrum of the dM8e star VB 10 (Allard & Hauschildt 1995a). The corresponding  $H^-$  continuum obtained by neglecting molecular opacities only in the radiative transfer (long dot-dashed) reveals the magnitude of these opacities in a typical late-type M dwarf. The Planck distribution of the same  $T_{eff}$  is also shown for comparison. From Allard et al. (1997).

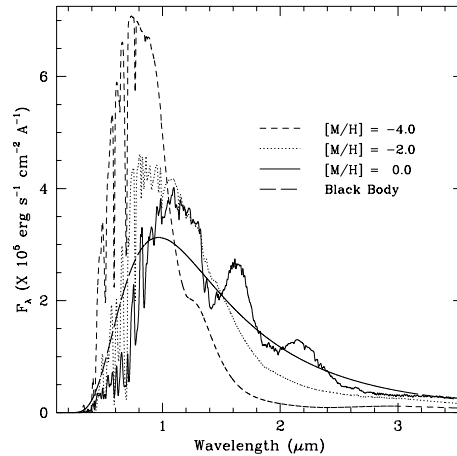


**Fig. 2.** Spectral distributions of emerging fluxes at the stellar surface for 3,000 K models with metallicities corresponding roughly to the solar neighborhood ( $[M/H] = 0.0$ ), halo ( $[M/H] = -2.0$ ), and Population III ( $[M/H] = -4.0$ ) stars. A black-body of the same effective temperature (smooth curve) is shown for comparison. From Allard et al. (1997).

These new observations have prompted further evolution of stellar atmosphere modeling and helped rejuvenate the field in general.

In the following we will briefly introduce the numerical methods that modern stellar atmosphere research employs (there are also plenty of legacy applications and codes that are still widely used) and then discuss some results that are of interest in the context of this meeting.

## 2. Methods and Models

For our model calculations, we use our multipurpose stellar atmosphere code PHOENIX (version 13.13 Hauschildt et al. (1997b); Baron & Hauschildt (1998); Hauschildt et al. (1999a,b); Hauschildt & Baron (1999). Details of the numerical methods are given in the above references, so we do not repeat the description here.

### 2.1. Line opacities

One of the most important recent improvements of cool stellar atmosphere models is the treatment of molecular line opacity. Our combined molecular line list includes about 550 million molecular lines. The lines are selected for every model from the master line list at the beginning of each model iteration to account for changes in the model structure (see below). Both atomic and molecular lines are treated with a direct opacity sampling method (dOS). We do *not* use pre-computed opacity sampling tables, but instead dynamically select the relevant LTE background lines from master line lists at the beginning of each iteration for every model and sum the contribution of every line within a search window to compute the total line opacity at *arbitrary* wavelength points. The latter feature is crucial in NLTE calculations in which the wavelength grid is both irregular and variable from iteration to iteration due to changes in the physical conditions. This approach also allows detailed and depth dependent line profiles to be used

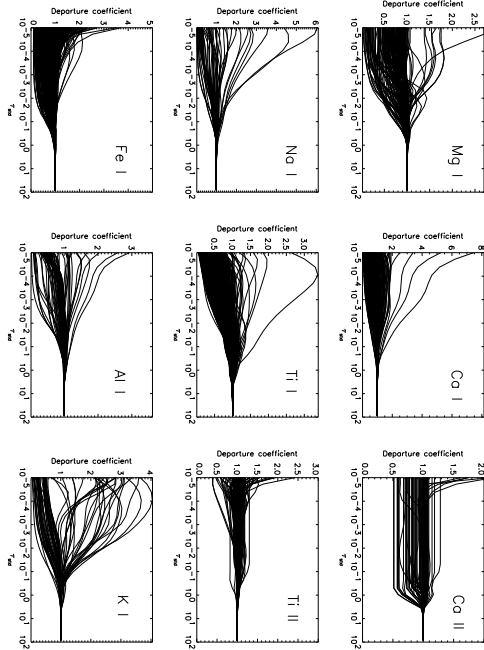


**Fig. 3.** Overview over selected departure coefficients for a NLTE model with  $T_{eff} = 4000$  K,  $\log g = 0.0$ , and solar abundances.

during the iterations. Although the direct line treatment seems at first glance computationally prohibitive, it leads to more accurate models. This is due to the fact that the line forming regions in cool stars and planets span a huge range in pressure and temperature so that the line wings form in very different layers than the line cores. Therefore, the physics of the line formation is best modeled by an approach that treats the variation of the line profile and the level excitation as accurately as possible. To make this method computationally more efficient, we employ modern numerical techniques, e.g., vectorized and parallelized block algorithms with high data locality (Hauschildt et al. 1997b), and we use high-end workstations or parallel supercomputers for the model calculations.

In the calculations presented in this contribution, we have included a constant statistical velocity field,  $\xi = 2 \text{ km s}^{-1}$ , which is treated like a microturbulence. The choice of lines is

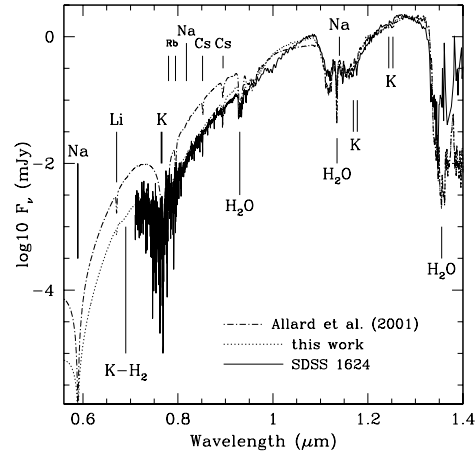


**Fig. 4.** Synthetic spectra obtained with the van der Waals approximation (dot-dashed line), and with the detailed profiles of Fig 3 (dotted line) are compared for an effective temperature of 1000 K, surface gravity of  $\log g = 5.5$ , and solar composition. The observed spectrum of SDSS 1624 (full line) is also shown. The synthetic spectra have been degraded to a  $10 \text{ \AA}$  resolution throughout, and the models are converged.

dictated by whether they are stronger than a threshold  $\Gamma \equiv \chi_l / \kappa_c = 10^{-4}$ , where  $\chi_l$  is the extinction coefficient of the line at the line center and  $\kappa_c$  is the local b-f absorption coefficient (see Hauschildt et al. (1999b), for details of the line selection process). This typically leads to about 10 – 250 million lines which are selected from master line lists, depending on model parameters. The profiles of these lines are assumed to be depth-dependent Voigt or Doppler profiles (for very weak lines). Details of the computation of the damping constants and the line profiles are given in Schweitzer et al. (1996). We have determined by test calculations that the details of the line profiles and the threshold  $\Gamma$  do not have a significant effect on either the model structure or the synthetic spectra. In addition, we include about 2000 photo-ionization cross sections for atoms

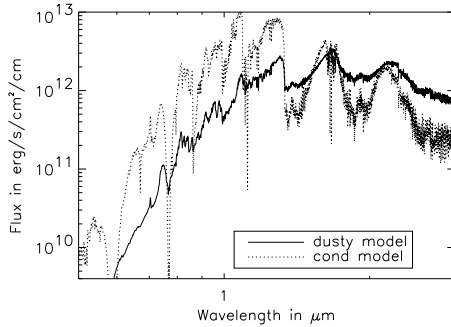


**Fig. 5.** This plot shows the difference between synthetic spectra calculated for a model atmospheres assuming complete settling of all formed dust particles below the layers where spectrum forms (“cond” model) and for a model that assumes that the dust particles remain close to the layer in which they formed (“dusty” model) for  $T_{eff} = 1700$  K,  $\log g = 4.5$  and solar abundances.

and ions (Mathisen 1984; Verner & Yakovlev 1995).

## 2.2. Equation of State

The equation of state (EOS) is an enlarged and enhanced version of the EOS used in Allard et al. (1997). We include about 500 species (atoms, ions and molecules) in the EOS. This set of EOS species was determined in test calculations. The EOS calculations themselves follow the method discussed in AH95. For effective temperatures,  $T_{eff} < 2500$  K, the formation of dust particles has to be considered in the EOS. In our models we allow for the formation (and dissolution) of a variety of grain species.

## 2.3. Non-LTE

The NLTE treatment of large model atoms or molecules such as  $H_2O$  and  $TiO$  which have several million transitions is a formidable problem which requires an efficient method for the numerical solution of the multi-level NLTE radiative transfer problem. Classical techniques, such as the complete linearization or the Equivalent Two Level Atom method, are

computationally prohibitive for large model atoms and molecules. Currently, the operator splitting or approximate  $\Lambda$ -operator iteration (ALI) method (e.g., Cannon (1973); Rybicki (1972, 1984); Scharmer (1984) seems to be the most effective way of treating complex NLTE radiative transfer and rate equation problems. Variants of the ALI method have been developed to handle complex model atoms, e.g., Anderson’s multi-group scheme (Anderson 1987, 1989) or extensions of the opacity distribution function method (Hubeny & Lanz 1995). However, these methods have problems if line overlaps are complex or if the line opacity changes rapidly with optical depth, a situation which occurs in cool stellar atmospheres. The ALI rate operator formalism (Hauschildt 1993; Hauschildt & Baron 1999), on the other hand, has been used successfully to treat very large model atoms such as Fe directly and efficiently (cf. Hauschildt et al. (1996); Baron et al. (1996); Hauschildt & Baron (1999)).

## 3. Results

In the following sections we will give a few representative results that highlight important new developments in stellar atmospheres.

### 3.1. Line blanketing

The number of molecular lines that are important in M dwarf (and later) atmospheres is quite large. About 215 million molecular lines are selected (see above) for a typical giant model with  $T_{eff} \approx 3000$  K whereas about 130 million molecular lines have to be considered for a dwarf model with the same effective temperature. The large “density” (in wavelength space) of molecular lines causes large line blanketing effects as illustrated in Fig. 1 for a very simple case. The nearly complete coverage of the optical spectrum by  $TiO$  lines and of the near IR spectrum by  $H_2O$  lines effectively locks the peak of the spectral energy distribution in place at around  $1.1 \mu m$  even for substantially different  $T_{eff}$ , in stark contrast to the behavior expected for blackbodies. Line blanketing also produces a strong metallicity effect on the spectra as illustrated in Fig. 2. Lowering the

metal abundances reduces both the TiO and H<sub>2</sub>O opacities by roughly the same amount. However, the H<sub>2</sub>O opacity in the near IR is replaced by increasingly (with lower metallicity) stronger collision induced opacities (due to the larger pressures in the spectrum forming regions). Therefore, the spectrum gets *bluer* with lower metallicities, even for comparatively low effective temperatures.

### 3.2. NLTE effects

Due to their very low electron temperatures, the electron density is extremely low in M stars; absolute electron densities are even lower than found in low density atmospheres, such as those of novae and SNe. Collisional rates due to collisions with electrons, which tend to restore LTE, are thus very small in cool stars. This in turn could significantly increase the importance of NLTE effects in M stars when compared to, e.g., solar type stars with much higher electron densities and temperatures. Collisions with molecular hydrogen and helium will at least partly compensate for the diminished electron collisions, but cross-sections for these processes are not very well known. Therefore, the assumption of LTE for atoms and molecules in cool stars is by no means certain and needs to be verified for each species individually. We have performed test calculations to place an upper limit for the importance of atomic NLTE effects in cool stars by only considering electron collisions.

We have calculated a small number of NLTE models in order to investigate the importance of NLTE effects on the structure of the model atmospheres. The results for cooler models were discussed in Hauschildt et al. (1997a) and are not repeated here. Figure 3 shows an overview of selected NLTE species for models with  $T_{eff} = 4000$  K,  $\log g = 0.0$  and solar abundances. The total number of NLTE levels in each model is 4532 with a total of 47993 primary NLTE lines (see Hauschildt & Baron (1999) and references therein for details). For most of the species, the departure coefficients are always close to unity, in particular for species with resonance lines and photoionization edges in the UV part of the

spectrum. The species shown in Figure 3 are species with the most pronounced departures from LTE. The departures are generally too small to significantly affect the structure of the atmospheres. Results for NLTE calculations for the CO molecule show that the high cross-sections of H<sub>2</sub> and He collisions restore LTE very successfully in the case of dwarf stars (Schweitzer et al. 2000).

### 3.3. Dust and cloud formation

The effects of dust formation on the atmosphere are mainly (a) the removal of important opacity sources (e.g., TiO, VO) from the gas phase and a corresponding weakening of their spectral lines; and (b) the presence of additional opacities produced by the grains themselves, cf. Fig. 5. The latter depends on the behavior of the macroscopic dust particles:

- a) They might remain as dust clouds in the layers where the dust originally formed and thus cause strong optical and IR opacities due to these clouds (“Dusty” models).
- b) They could rain out and settle below the line and continuum forming regions, resulting in no grain opacities detectable in the spectrum (“Cond” models).
- c) They can form depleted clouds in the atmosphere so that dust opacities would only be present in the cloud layers but not necessarily in all the layers where the dust had originally formed (“Settle” models).

Observational evidence (see below) suggests that case (a) is realized for  $T_{eff} > 1800$  K (late M dwarfs to early L dwarfs) whereas for giant planets and extreme T dwarfs case (b) appears to be more appropriate. In the intermediate regime, partial clouds appear to form and case (c) must be investigated. At the present time, this sequence is still very tentative and the physical models of dust and cloud formation have to be refined to obtain a truly physical picture of brown dwarfs and extrasolar giant planets.

### 3.4. Line Profiles

Allard et al. (2003) discusses a unified theory of spectral line broadening to calculate neutral atom spectra given the interaction and radiative transition moments for relevant states of the radiating atom with other atoms in its environment. Complete details and the derivation of the theory are given by Allard et al. (1999). The alkali line profiles and satellites are calculated for physical conditions encountered in the atmospheres of brown dwarfs. Although our theory takes into account the effects of multiple close collisions, for use here we computed the line profile by using the low density approximation as described by Allard et al. (1994). This approximation uses the expansion of the autocorrelation function in powers of density and we restricted our expansion to the first order. We have assumed that interactions of an absorbing atom with more than one perturber do not contribute to the far line wing profile. To illustrate the effects of the individual line profiles, we have computed model atmospheres and synthetic spectra using the new theoretical Na I D and K I profiles. The results are compared to previous models in Fig 4, and demonstrate that these improvements are of *fundamental* importance for obtaining a better quantitative interpretation of the spectra, also concluded by BV. The new profiles carry significantly more opacity within the first 1800 Å from the line centers, while providing less opacity further in the red wings. The optical-to-red pseudo-continuum is, therefore, depressed, while raised at the flux maximum near 1.1 μm, compared to models based upon the van der Waals approximation. Fig 4 also shows the observed spectrum of the T6 methane brown dwarf SDSS 1624. Although no attempt has been made to adjust the atmospheric parameters, the changes provided by the new profiles correspond more closely to the strongly depressed red spectrum of this brown dwarf.

#### 4. Summary and Conclusions

In this paper we have discussed a few new results of stellar atmosphere modeling that have helped to resolve some outstanding problems understanding and interpreting observed stel-

lar spectra. During the last decade, progress was made by breakthroughs in both methodology and computer technology, which has lead to substantially improved models and synthetic spectra. In many cases, even our currently “best effort” models cannot reproduce observed spectra satisfactorily, this is in particular the case for L and T dwarfs. However, this is due to physical effects that we “know” but we cannot currently describe well enough (e.g., incomplete line lists for key molecules or dust and cloud formation processes). Another area that requires much more work is our detailed understanding of winds from both hot and cool stars. There is currently a lot of effort being put into the solution of these key problems, although it is clear that once they are solved, others will pop up in unexpected places.

*Acknowledgements.* This work was supported in part by NASA grants NAG 5-8425 and NAG 5-3619 to the University of Georgia and by NASA grant NAG5-3505, NSF grants AST-0204771 and AST-0307323, and an IBM SUR grant to the University of Oklahoma. PHH was supported in part by the Pôle Scientifique de Modélisation Numérique at ENS-Lyon. Some of the calculations presented here were performed at the San Diego Supercomputer Center (SDSC), supported by the NSF, at the National Energy Research Supercomputer Center (NERSC), supported by the U.S. DOE, and at the Höchstleistungs Rechenzentrum Nord (HLRN). We thank all these institutions for a generous allocation of computer time.

#### References

- Allard, F., & Hauschildt, P. H. 1995a, in *The Bottom of the Main Sequence - and Beyond*, ed. C. Tinney, ESO Astrophysics Symposia (Springer-Verlag Berlin Heidelberg), 32–44
- Allard, F., & Hauschildt, P. H. 1995b, *ApJ*, 445, 433
- Allard, F., Hauschildt, P. H., Alexander, D. R., & Starrfield, S. 1997, *ARAA*, 35, 137
- Allard, N. F., Allard, F., Hauschildt, P. H., Kielkopf, J. F., & Machin, L. 2003, *A&A*, 411, L473
- Allard, N. F., Koester, D., Feautrier, N., & Spielfiedel, A. 1994, *A&AS*, 108, 417
- Allard, N. F., Royer, A., Kielkopf, J. F., & Feautrier, N. 1999, *Phys. Rev. A*, 60, 1021

- Anderson, L. S. 1987, in *Numerical Radiative Transfer*, ed. W. Kalkofen (Cambridge University Press), 163
- Anderson, L. S. 1989, *ApJ*, 339, 559
- Baron, E., & Hauschildt, P. H. 1998, *ApJ*, 495, 370
- Baron, E., Hauschildt, P. H., Nugent, P., & Branch, D. 1996, *MNRAS*, 283, 297
- Cannon, C. J. 1973, *JQSRT*, 13, 627
- Hauschildt, P., Allard, F., Ferguson, J., Baron, E., & Alexander, D. R. 1999a, *ApJ*, 525, 871
- Hauschildt, P., Baron, E., Starrfield, S., & Allard, F. 1996, *ApJ*, 462, 386
- Hauschildt, P. H. 1993, *JQSRT*, 50, 301
- Hauschildt, P. H., Allard, F., Alexander, D. R., & Baron, E. 1997a, *ApJ*, 488, 428
- Hauschildt, P. H., Allard, F., & Baron, E. 1999b, *ApJ*, 512, 377
- Hauschildt, P. H., & Baron, E. 1995, *JQSRT*, 54, 987
- Hauschildt, P. H., & Baron, E. 1999, *Journal of Computational and Applied Mathematics*, 102, 41
- Hauschildt, P. H., Baron, E., & Allard, F. 1997b, *ApJ*, 483, 390
- Hubeny, I., & Lanz, T. 1995, *ApJ*, 439, 875
- Mathisen, R. 1984, *Photo Cross-sections for Stellar Atmosphere Calculations — Compilation of References and Data*, Inst. of Theoret. Astrophys. Univ. of Oslo, Publ. Series No. 1.
- Rybicki, G. B. 1972, in *Line Formation in the Presence of Magnetic Fields*, ed. G. Athay, L. L. House, & G. Newkirk Jr. (Boulder: High Altitude Observatory), 145
- Rybicki, G. B. 1984, in *Methods in Radiative Transfer*, ed. W. Kalkofen (Cambridge Univ. Press), 21
- Scharmer, G. B. 1984, in *Methods in Radiative Transfer*, ed. W. Kalkofen (Cambridge Univ. Press), 173
- Schweitzer, A., Hauschildt, P. H., Allard, F., & Basri, G. 1996, *MNRAS*, 283, 821
- Schweitzer, S., Hauschildt, P. H., & Baron, E. 2000, *ApJ*, 541, 1004
- Verner, D. A., & Yakovlev, D. G. 1995, *A&AS*, 109, 125